Macromolecules

ARTICLE

pubs.acs.org/Macromolecules

Tuning of the Elastic Modulus of Polyelectrolyte Multilayer Films built up from Polyanions Mixture.

K. Trenkenschuh,[†] J. Erath,[†] V. Kuznetsov,[†] J. Gensel,[†] F. Boulmedais,[*,‡] P. Schaaf,[‡,§,∥] G. Papastavrou,[†] and A. Fery[*,†]

[†]Department of Physical Chemistry II, University of Bayreuth, Universitätsstrasse 30, 95440, Bayreuth, Germany

[‡]Institut Charles Sadron, Centre National de la Recherche Scientifique (UPR 22), Université de Strasbourg, 23 rue du Loess, 67034 Strasbourg, France

[§]Ecole Européenne de Chimie, Polymères et Matériaux, Université de Strasbourg, 25 rue Becquerel, 67087 Strasbourg, France

[∥]International Center for Frontier Research in Chemistry, 8 allée Gaspard Monge, 67083 Strasbourg, France

ABSTRACT: In this paper, we report on the mechanical characterization of polyelectrolytes multilayer (PEM) films prepared from poly(glutamic acid)−poly(styrenesulfonate) (PGA−PSS) blends, deposited in alternated spray deposition with poly(allylamine hydrochloride) (PAH). The polyanion composition of the blended film was first investigated by Fourier transformed infrared spectroscopy in the attenuated total reflection mode. The monomer molar fraction of PGA in the film increases almost linearly with x, i.e., the monomer molar fraction of PGA in the sprayed polyanion solution. The mechanical properties of the blended $(PAH/PGA_x\text{-}PSS_{1-x})_n$ film were measured using two methods: (i) the wrinkling metrology method and (ii) by colloidal probe atomic force microscopy. We demonstrate that Young's modulus of the $PAH/PGA_x\text{-}PSS_{1-x}$ multilayer films can be systematically controlled by the chemical composition of these films, depending on x. Measurements indicate that increasing the monomer molar fraction of PGA in the blended film results in a decrease in film modulus up to 2 orders of magnitude as compared to the PAH/PSS system. At a monomer molar fraction of PGA in the film around $x = 0.7$, this system undergoes such a transition. We also show that for a given x the elastic properties of these films are significantly affected by the humidity conditions. For a $(PAH/PGA_{0.88}\text{-}PSS_{0.12})$ film, Young's modulus of the film varies from several hundred to few MPa by solely altering the relative humidity between 12.5% and 80%.

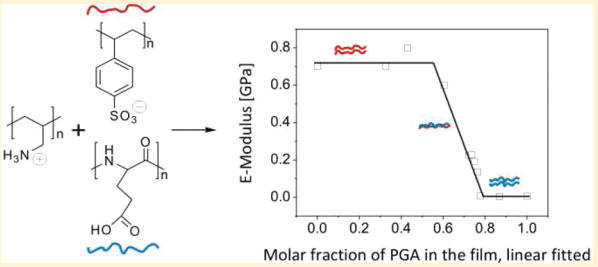

INTRODUCTION

Polyelectrolyte multilayer (PEM) films prepared by the layer-by-layer (LbL) technique became very popular since the concept was introduced by Decher et al. in the early 1990s.[1] The method relies on the sequential adsorption of oppositely charged polyelectrolytes to construct thin multilayered films. The adsorption results in charge overcompensation after each polyelectrolyte deposition. This allows the alternated assembly of oppositely charged polyelectrolytes. Numerous polymeric materials with different functional groups are available for the multilayer construction which resulted in numerous applications such as controlling wetting properties or interactions with biological systems,[2] anticorrosion coatings,[3−5] free-standing membranes,[6−10] osmotic pressure sensors,[11] and to build up micro- and nanocapsules.[12,13] Adjusting mechanical properties of PEMs is desirable for most applications mentioned above. This can be achieved within a limited range by variation of solution conditions during adsorption (pH,[14,15] ionic strength[16]), by changing the molecular weight of used polyelectrolytes,[17] by cross-linking of the film,[18,19] or by adding a linear growing capping multilayer films on an exponential growing one.[20] In order to tune mechanical properties over many orders of magnitude using the same chemical building blocks, synthetic approaches relying on the use of random copolymers of controlled ratio of charged and uncharged monomers have been used.[21−23] It has been also shown that the elastic modulus of PEM films can be significantly affected by changing the ambient relative humidity (RH).[24]

Using blends of polyanions[25−31] or polycations[32,33] as building blocks provides a potentially interesting alternative to tune several properties of PEMs without synthesis of novel molecular compounds. To control the mechanical property of PEMs, our approach relies on using blends of components, which are known to result in very different mechanical properties where pure components are used. We study LbL films prepared with weakly charged poly(allylamine hydrochloride) (PAH) and two polyanions, poly(styrenesulfonate, sodium salt) (PSS) and a polypeptide poly(L-glutamic acid, sodium salt) (PGA). Our motivation is to investigate the effect of polyanion mixing ratio and the humidity on the mechanical properties since in the literature a huge difference in elastic modulus of $(PAH/PSS)_n$ and $(PAH/PGA)_n$ films is reported. In previous work, Young's modulus of PAH/PSS capsules was estimated to be between

Received: August 29, 2011
Revised: October 12, 2011
Published: October 28, 2011

1.3 and 1.9 GPa.[34] Nolte et al. reported for the PAH/PSS multilayer system a modulus of 2.7 ± 0.3 GPa[24] and Gao et al., who measured hollow polyelectrolyte capsules, found that Young's modulus for the PAH/PSS system ranges between 500 and 700 MPa.[35] Boudou et al. reported for the PAH/PGA system the elastic constant value of 118 ± 34 kPa as determined by AFM nanoindentation in liquid environment.[19]

In this study, we show that the different properties of these two polyanions, PGA and PSS, strongly affects the elasticity of the blended PAH/PGA_x-PSS_{1-x} PEM films, with x representing the molar fraction of the monomer repeat unit of PGA in the polyanion solution. We find a dramatic decrease and a sharp transition in the film modulus as a function of molar fraction of PGA in the film. This behavior is remarkable, because for many systems preferential adsorption of one compound shifts transitions in physical properties of multilayers to extreme compositions.[26−28,30−32,36] Examples where transition occur at moderate ratios are rare.[27] Furthermore, we demonstrate that we can tune the mechanical properties by altering the relative humidity.

MATERIALS AND METHODS

Materials. For the preparation of the $(PAH/PGA_x\text{-}PSS_{1-x})_n$ multilayer architectures, the following commercially available polyelectrolytes were used: Poly(allylamine hydrochloride) (PAH, M_W = 56 000 g mol^{-1}, CAS 71550−12−4; cat. no. 28,322−3), poly(styrenesulfonate, sodium salt) (PSS, M_W = 70 000 g mol^{-1}, CAS 25704−18−1; cat. no. 24,305−1), poly(L-glutamic acid, sodium salt) (PGA, M_W = 15 000 g mol^{-1}, CAS 26247−79−0; cat. no. P-4761) and branched poly(ethylene imine) (PEI, M_W = 750 000 g mol^{-1}, 50 wt % in H_2O, CAS 9002−98−6; cat. no. 18,197−8). All polyelectrolytes were purchased from Sigma-Aldrich and were used without further purification. Figure 1 shows the polyelectrolytes used in this study.

Solutions of Polyelectrolytes. The polyelectrolyte solutions were prepared by dissolving the appropriate amounts of polyelectrolytes in filtered (0.20 μm Carl Roth) 0.15 M aqueous sodium chloride (NaCl, Riedel-de Haën) solutions. Millipore water (resistivity =18.2 MΩ cm) was used in all experiments. The pH of all the solutions was adjusted to pH 7.4 by addition of appropriate volumes of either HCl solution (Grüssing GmbH Analytika, Germany) or NaOH solution (Grüssing GmbH Analytika, Germany) immediately before measurement. The $(PAH/PGA_x\text{-}PSS_{1-x})_n$ films were constructed by using a 1 mg mL^{-1} PAH solution as polycation and a polyanion solution obtained by mixing x mL of a 0.733 mg mL^{-1} PGA solution and $(1 - x)$ mL of a 1 mg mL^{-1} solution of PSS (x represents the molar percentage of the monomer repeat unit of PGA). The mixed PGA_x-PSS_{1-x} solution thus has a total monomer repeat unit concentration of 4.85 × 10^{-3} mol L^{-1}.

Substrate Preparation. To determine the mechnanical properties of PEM films, colloidal probe atomic force microscopy (CP-AFM), and wrinkling metrology (WM) method were used. For the CP method, substrates of silicon wafers (CrysTec) were cleaned as follows: first, the substrates were immersed for at least 1 h in the 0.15 M NaCl aqueous solution at pH 7.4. Then the surfaces were immersed in 1 mg mL^{-1} PEI solution for 10 min. The substrates were then rinsed 10 min with 0.15 M NaCl aqueous solution. For the WM method, poly(dimethylsiloxane) (PDMS) sheets (a typical elastomer) with thicknesses of ∼2 mm were prepared by mixing the curing agent and base monomer (Sylgard 184, Dow Corning, USA) with 1:10 weight ratio. The mixture was stirred and filled in a carefully cleaned, plain glass dish.[37] After 24 h degassing at room temperature and curing at 60 °C for 3 h in an oven, the cross-linked PDMS was cut into 40 × 10 mm stripes. In order to facilitate the multilayer assembly the surfaces of PDMS sheets were first hydrophilized (PDMS sheets were exposed for 2 min to air plasma at 0.1 mbar using a plasma etcher operating at 1 W (Flecto10, Plasma Technology, Germany)) and then immersed in 1 mg mL^{-1} PEI solution for 30 min.

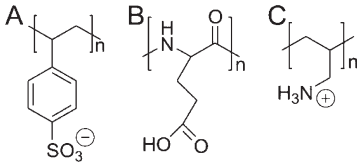

Figure 1. Chemical structures of the polyelectrolytes used in this study: the two polyanions (A) PSS, (B) PGA, and the polycation (C) PAH.

PEM Film Preparation by Spray Coating. The PEM films were assembled on silicon wafers and on plasma treated (see above) PDMS sheets by the spray coating method.[38,39] The PEI-coated substrates were placed vertically in a homemade spray unit to allow liquid drainage along their surfaces. The appropriate polyelectrolyte solutions were filled into spray bottles (30 mL, NeoLab Migge GmbH, Germany) which were manually pressurized twice for each deposition step. After each step, the polymer was sprayed for 10 s followed by a rinsing step with water for 3 s (200 mL spray bottles "air boy", Carl Roth GmbH, Germany) to rinse the surface. The films were dried in a stream of nitrogen before characterization.[21]

Characterization Methods. *Ellipsometry.* Layer thicknesses of the multilayers grown on silicon wafers and on PDMS substrates were determined with a Sentech SE 850 spectroscopic ellipsometer at a fixed incidence angle of 70° (on silicon wafers) and of 40° (on PDMS substrates). Measurements were done at wavelength range between 400 and 800 nm. Layer thicknesses on transparent PDMS substrates were determined using a Cauchy dispersion relationship.[40,41] To calculate the film thicknesses, we used a three-layer model with layer 1, hydrophilized PDMS substrate (n = 1.41), layer 2, PEM film (n = 1.52), and layer 3, air (n = 1.00). For each sample, at least three spots were measured and averaged and the results were cross-checked with AFM.

Optical Microscopy. Optical microscopy images of the wrinkled surfaces were recorded using an inverted Zeiss Axiovert 200 (Zeiss, Jena) microscope with a Zeiss Achroplan 20 × /0.45 objective. The microscope was connected to a digital camera (AxioCam HRm, Zeiss) for quantitative data acquisition.

Colloidal Probe Atomic Force Microscopy. The mechanical properties of the samples with PGA_x-PSS_{1-x} polyanion mixtures, where x ranges from 0.71 to 1 were investigated by force−distance measurements using the colloidal probe technique.[42,43] Under ambient conditions, force curves were recorded with a Nanowizard AFM (JPK instrument, Berlin). We used a tipples cantilever (NSC12, Micromash, USA) with Si-colloidal probe (Bang laboratories, USA) prepared using Optical adhesive Norland 63 (for cured glue E = 1.65 GPa) with a radius of R = 3.4 μm and a spring constant of 0.257 N/m. The spring constant k was determined by the thermal noise method, introduced by Hutter and Bechhoefer.[44]

To investigate the influence of humidity on the mechanical properties of PEM, an Asylum MFP 3D AFM was used with an Asylum Humidity control cell. The humidity is maintained by injecting saturated salt solutions, which determine the water vapor pressure in the chamber (relative humidities are 84−85% (KCl_{sat}), 33% ($MgCl_{2,sat}$) and 8−9% (KOH_{sat}) in the temperature range of 20−25 °C[45,46]). The sample was fixed with double-sided adhesive over the area of ca. 1.1 cm^2 that has a negligible effect on the indentation of a film with E = (8−900) MPa. Colloidal probes with R = 3.4 μm and R = 2.3 μm were prepared by gluing Silica-particles (Bang laboratories, USA) with Optical adhesive Norland 63 (for cured glue E = 1.65 GPa) to tipless silicon cantilevers (NSC12, Mikromasch, USA, k = 0.25 and 0.77 N/m). Cantilevers were calibrated by Hutter and Bechhoefer method.[44] Data analysis was carried

dx.doi.org/10.1021/ma201974g |Macromolecules 2011, 44, 8954–8961

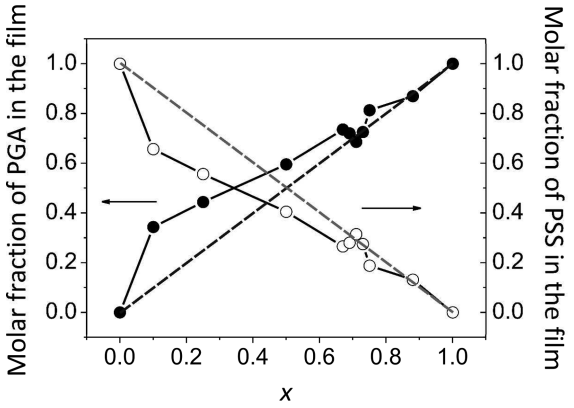

Figure 2. Evolution of the monomer molar fractions of PGA (closed circle) and of PSS (open circle) in the $(PAH/PGA_x\text{-}PSS_{1-x})_n$ blended film as a function of x, the monomer molar fraction of PGA in solution used for the buildup by alternated contact with a polyanion PGA and PSS mixture and a PAH solutions. The dashed line corresponds to the ideal partitioning of PGA (black) and PSS (gray) between the solution and the film. These data where obtained from films with a thickness of 80 ± 10 nm. The evolution of molar fraction of PGA in the film can be fitted by a linear function for $0.1 < x < 1$ with a slope of 0.7.

out by Asylum MFP 3D build-in software (v. 10102010) for nanoindentation.

Fourier Transform Infrared Spectroscopy in the Attenuated Total Reflection Mode (ATR-FTIR). The Fourier Transform Infrared (FTIR) experiments were performed on a Vertex 70 spectrometer (Bruker, Germany) using DTGS detector. The spectra relative to the multilayers were determined in the Attenuated Total Reflection (ATR) mode using a 45° trapezoidal ZnSe (internal reflection element) crystal (6 reflections, dimensions 72 × 10 × 6 mm^3) in ATR cell (GRASEBY-SPECAC, England). Reference (bare ZnSe crystal) and sample spectra were taken by collecting 128 interferograms between 800 and 4000 cm^{-1} at 2 cm^{-1} resolution, using Blackman-Harris three-term apodization and the standard Bruker OPUS/IR software (version 5.0). The PEM films were assembled on ZnSe crystal by the spray coating method described above. All the sample spectra, as for the reference, were recorded with the ZnSe crystal in contact with air.

To estimate the molar percentage of monomer of PGA and PSS in the $(PAH/PGA_x\text{-}PSS_{1-x})_n$ films, we performed calibration curves in order to correlate the absorbance with concentration of pure polyelectrolyte. The PGA and PSS were dissolved in deuterated solution of 150 mM NaCl at pH 7.4. D_2O was used as solvent instead of water because the amide I band of PGA is affected by the strong absorption of water around 1643 cm^{-1} (O−H bending), whereas the corresponding vibration in D_2O is found at around 1209 cm^{-1}. IR spectra of PGA and PSS solutions were acquired using Bruker Vector 70 FTIR spectrometer with Platinum ATR accessory that contained a diamond crystal (Bruker Optics, USA).

RESULTS AND DISCUSSION

Buildup and Film Composition of $(PAH/PGA_x\text{-}PSS_{1-x})_n$ Films. We focused on the system $(PAH/PGA_x\text{-}PSS_{1-x})_n$ because it is known, that the elastic modulus of multilayer films constructed from pure PSS solution and PAH resides in GPa region[24,34] whereas films built up from pure PGA solution and PAH exhibit an elastic modulus in the kPa range.[19] The buildup of $(PAH/PGA_x\text{-}PSS_{1-x})_n$ films was studied previously.[25] It was shown that the growth regime of this film is changing from exponential to linear by adjusting monomer molar fraction of PGA in solution. Indeed, pure PAH/PSS and pure PAH/PGA show linear and exponential film growth, respectively. To examine the mechanical properties of $(PAH/PGA_x\text{-}PSS_{1-x})_n$ multilayer films, the spray coating technique was used by systematically tuning x, monomer molar fraction of PGA in the polyanion sprayed solution.

Table 1. Monomer Molar Fraction of PGA in the Polyanion Solution, Number of Bilayers and Corresponding Film Thickness of $(PAH/PGA_x\text{-}PSS_{1-x})_n$ Multilayer Films Prepared with 0.15 M NaCl at pH 7.4

PGA molar fraction in solution (x)	number of bilayers (n)	thickness (nm)[a]
0	32	095.3 ± 7.0
0.10	30	107.8 ± 3.6
0.25	21	111.2 ± 8.7
0.50	12	115.5 ± 3.1
0.67	11	112.4 ± 6.3
0.69	11	102.5 ± 7.8
0.71	11	094.5 ± 4.1
0.73	11	094.4 ± 6.0
0.75	25	521.4 ± 2.9
0.88	25	544.5 ± 7.9
1.00	23	505.4 ± 4.8

[a] Determined by ellipsometry.

To investigate the relative composition of PGA and PSS inside the $(PAH/PGA_x\text{-}PSS_{1-x})_n$ film as a function of x, we performed FTIR measurements. We first performed calibration curves aimed at correlating the absorbance with concentration of pure PGA and PSS polyelectrolytes. At a wavenumber of 1567 cm^{-1} corresponding to the carboxylic band,[47−49] we obtained an apparent extinction coefficient of 7.9×10^{-2} M^{-1} in monomer of PGA. In the case of PSS, we obtained apparent extinction coefficients of 7.2×10^{-2} and 7.8×10^{-2} M^{-1} in monomer of PSS respectively at the wavelengths of 1009 and 1037 cm^{-1}, characteristic bands of PSS.[50−52] We then performed FTIR-ATR spectroscopy on $(PAH/PGA_x\text{-}PSS_{1-x})_n$ films for x varying from 0 to 1. It has to be noted that, for all the experiments performed, the films were built to reach a thickness of (80 ± 10) nm in the dry state, which is significantly smaller than the penetration depth of the evanescent wave (600 nm at 1000 cm^{-1}). By measuring after baseline subtraction the absorbance of PGA and PSS in the films, we calculated the molar concentrations of PGA and PSS monomers using the extinction coefficients from the calibration curves.

Figure 2 shows the monomer molar fraction of PGA and PSS in the film as a function of monomer molar fraction of PGA in the polyanion solution. A strong adsorption preference of PGA is found especially for $x \leq 0.5$. Such a preferential adsorption was also found in the case of PSS/DNA-PAH,[28] poly(aspartic acid)/PGA-poly(L-lysine)[26] and poly(4 vinylpyridine)/PAH mixtures.[32] Beyond $x = 0.5$, the film composition is close to the solution composition and follows then a linear behavior. The values obtained for $x = 0.67-0.73$ by FTIR could be more sensitive to errors due to sensitivity of the system. Therefore, we fitted the molar fraction in PGA in the film by a linear function for $0.1 < x < 1$ with a slope of 0.7 (Table 2).

On the basis of the polyelectrolytes and the tunable composition of $(PAH/PGA_x\text{-}PSS_{1-x})_n$ films, we expect a broad range of elastic constants (ranging from lower MPa region for pure PAH/PGA up to GPa region for pure PAH/PSS). However, the film thicknesses are set in the range of 100 nm. These requirements

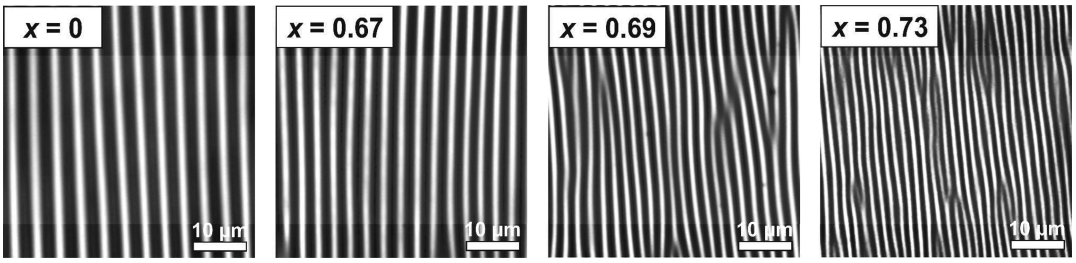

Figure 3. Optical microscopy images of wrinkled $(PAH/PGA_x\text{-}PSS_{1-x})_n$ multilayer films taken in the transmission mode; x ranges from 0 to 0.73. Samples prepared by stretching multilayer films coated PDMS slides by $\varepsilon = 2\%$ and releasing the strain.

are extremely challenging in terms of characterization techniques. To the best of our knowledge there is no single technique covering the whole range of elastic properties for this thin film regime. Therefore, we used two complementary techniques, the wrinkling method (WM) and the indentation technique (CP-AFM) in order to measure the full range of elastic constants. Wrinkling experiments allow us to analyze more rigid materials with moduli in the order of GPa down to several hundreds of MPa. In contrast, the CP - AFM technique is suitable for soft films with moduli of MPa until kPa range. For each technique, a minimum film thickness is required for reliable measurements. The number of $PAH/PGA_x\text{-}PSS_{1-x}$ bilayers was then tuned to obtain a sufficient thickness (Table 1).

High Modulus Regime: Wrinkling Metrology. The mechanical properties of $(PAH/PGA_x\text{-}PSS_{1-x})_n$ multilayer films, where x ranges from 0 to 0.73 were investigated with the sensitive technique named strain-induced elastic buckling instability for mechanical measurements (SIEBIMM) introduced by Stafford et al..[53] The basic idea of the buckling-based metrology is that a thin, stiff film coated onto an elastomeric substrate will buckle when subjected to planar compressive forces in order to relieve the strain energy in the system.

The wrinkling experiments were performed on a plasma-treated PDMS sheets with a hydrophilic surface. In order to minimize the influence of the silica surface layer on the buckling wavelength, plasma intensity and durations were kept at minimum. The film thicknesses of all samples were ca. 100 nm as recommended by Nolte et al. in order to minimize film thickness measuring errors.[41] Multilayer coated PDMS slides were stretched uniaxially in a customer-designed strain stage with the strains of only a few percent. The buckling wavelength, λ, was obtained after the subsequent relaxation of the specimens using optical microscopy. To determine the mechanical properties, the wavelength was evaluated via Fourier analysis of images using ImageJ.[54,55] The average wavelength was determined by collecting data from at least five locations on each sample. Knowing the wrinkling wavelength, λ, film thickness, d, and the modulus values of the PDMS substrates, E_s, (1.1 ± 0.1) MPa, determined using Universal Tester, Model 5565), the Young's modulus of the film, E_f, can be determined using eq 1:[53]

$$E_f = \frac{3E_s(1-\nu_f{}^2)}{1-\nu_s{}^2}\left(\frac{\lambda}{2\pi d_f}\right)^3 \qquad (1)$$

The Poisson's ratio of 0.33 was required for multilayers (ν_f), and a value of 0.5 was required for the elastomeric PDMS substrate (ν_s).[56]

The wrinkling experiments were carried out at the ambient RH of $(55 \pm 1)\%$. Figure 3 illustrates the optical microscopy images

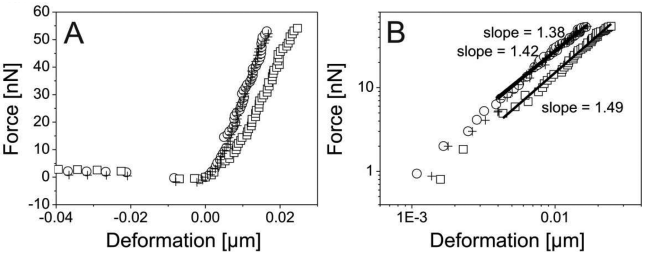

Figure 4. (A) Force vs deformation curves measured by AFM in approach for $(PAH/PGA_x\text{-}PSS_{1-x})_n$ multilayer films in a dry state, where $x = 0.75$ (○), $x = 0.88$ (□), and $x = 1$ (+). (B) Force vs deformation log−log profiles. The black lines represent a linear fit for deformations from 4 to 17 nm ($x = 0.75$ and $x = 1$) and from 4 to 25 nm ($x = 0.88$). The slopes of the fits in these ranges are 1.38 and 1.42 ($x = 0.75$ and $x = 1$) and 1.49 ($x = 0.88$), close to 3/2 as predicted by the Herzian power law.

of $(PAH/PGA_x\text{-}PSS_{1-x})_n$ multilayer films with x ranges from 0 to 0.73.

At the same film thickness, the wrinkling wavelength decreases from (3.6 ± 0.2) μm for $x = 0$ to (1.8 ± 0.1) μm for $x = 0.73$. According to the wavelength, the elastic modulus also decreases from (0.7 ± 0.2) GPa to (0.14 ± 0.09) GPa, respectively. The value of (0.7 ± 0.2) GPa for $x = 0$, i.e. pure PAH/PSS film, is comparable to those given in literature.[34,35]

Low Modulus Regime: AFM Technique. The Young's modulus of $(PAH/PGA_x\text{-}PSS_{1-x})_n$ films with x in the range of 0.75 to 1, which are too soft to be analyzed via the wrinkling method, was determined by indentation experiments with the colloidal probe.[57] The indentation experiments were performed on thick films (>500 nm) in order to reduce the substrate influence.[58] The indentation depths did not exceed 10% of the film thickness, which allows to neglect the substrate influence.[59] To determine the elastic modulus, the samples were measured at different lateral positions using the force-mapping mode. Measurements were performed on 20 different positions on a digital 100 μm^2 grid on the surface. The force−distance curves were analyzed using the JPK Image Processing software. To determine Young's modulus, the approach curve was fitted by the Hertz sphere model.[60]

Providing the following assumptions were matched by measuring with the colloidal probes, we used Hertz model for the fitting of force−indentation curves. The assumptions are as follows: (1) the indenter and indented sample are a linear elastic bodies. The sample is assumed to be an infinite half space, the indenter has spherical geometry; (2) the strains are small, i.e., the contact radius should be much smaller than the probe radius; (3) the indentation depth is less than 10% of the film

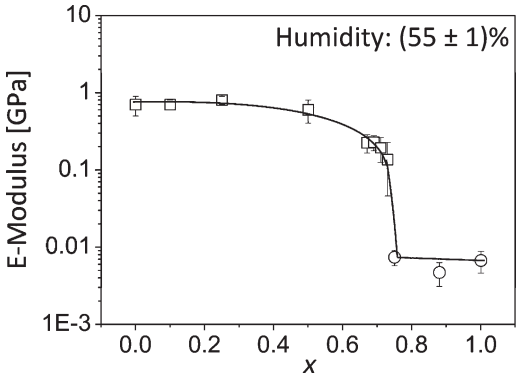

Figure 5. Elastic modulus E as a function of x, monomer molar fraction of PGA in the polyanion buildup solution. For x ranges from 0 to 0.73, E was deduced from wrinkling metrology measurements (□). For x ranges from 0.75 to 1, E was calculated from force vs deformation curves measured by colloidal probe AFM (○). The line is drawn to guide the eyes.

Table 2. x, Monomer Molar Fraction of PGA in the Polyanion Solution, the Corresponding Monomer Molar Fraction of PGA in the Film, Monomer Molar Fraction of PGA in the Film from the Linear Function and the Resulting Young's Modulus of $(PAH/PGA_x\text{-}PSS_{1-x})_n$ Multilayer Films Prepared with 0.15 M NaCl at pH 7.4

PGA molar fraction in solution (x)	PGA molar fraction in the film[a]	PGA molar fraction in the film from the linear function	Young's modulus (GPa)[b]
0	0	0	0.7 ± 0.2
0.10	0.34	0.33	0.7 ± 0.1
0.25	0.44	0.43	0.8 ± 0.1
0.50	0.60	0.60	0.6 ± 0.2
0.67	0.73	0.72	$(2.3 \pm 0.6) \times 10^{-1}$
0.69	0.72	0.74	$(2.3 \pm 0.5) \times 10^{-1}$
0.71	0.69	0.75	$(1.9 \pm 0.7) \times 10^{-1}$
0.73	0.72	0.76	$(1.4 \pm 0.9) \times 10^{-1}$
0.75	0.81	0.78	$(7.4 \pm 1.7) \times 10^{-3}$
0.88	0.87	0.87	$(4.7 \pm 1.6) \times 10^{-3}$
1.00	1	1	$(6.7 \pm 2.1) \times 10^{-3}$

[a] Determined by FTIR spectroscopy. [b] Determined by wrinkling metrology (x = 0−0.73) and by colloidal probe AFM (x = 0.75−1) at (55 ± 1)% of humidity.

thickness; (4) the surfaces are frictionless; (5) the adhesion is neglected.[61]

According to this model, the relation between Young's modulus (E), the force (F), and the deformation (δ) is

$$F = \frac{4}{3(1-\nu^2)} E R^{1/2} \delta^{3/2} \qquad (2)$$

where R is the radius of the sphere tip (3.4 μm) and ν is the Poisson ratio (0.33 for multilayers).

Figure 4 displays force-deformation curves measured in approach of the $(PAH/PGA_x\text{-}PSS_{1-x})_n$ films and the corresponding log−log profiles of these curves for x = 0.75, x = 0.88 and x = 1.

In the log−log plot the experimental data are correctly fitted by linear curves with slopes of about 1.5 which is in good

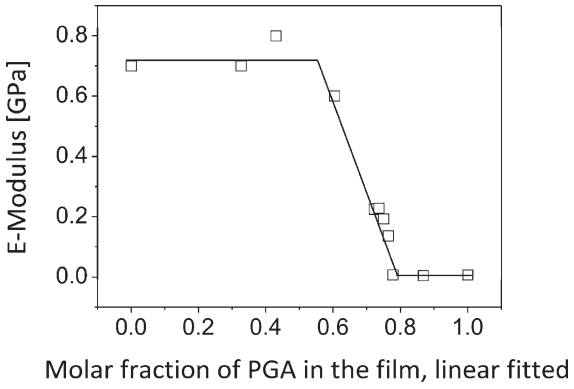

Figure 6. Young's modulus of $(PAH/PGA_x\text{-}PSS_{1-x})_n$ blended film as a function of the linear fitted monomer molar fraction of PGA in the film for $0.1 \leq x \leq 1$.

agreement with the scaling law predicted by Hertz model.[60] Although the assumption (5) was not strictly matched, the power law of force vs indentation was around 1.5 for the spherical indenter that clearly indicated the applicability of the Hertz model. Moreover, the use of this model is very common to estimate Young's modulus of elastic material from the force vs deformation experiments.[58,62,63]

The average Young's moduli determined according to the Hertz model (eq 2) are (7.4 ± 1.7) MPa, (4.7 ± 1.6) MPa, and (6.7 ± 2.1) MPa for $(PAH/PGA_x\text{-}PSS_{1-x})_n$ films prepared respectively with for x = 0.75, x = 0.88 and x = 1. The indentation experiments were carried out at the ambient RH of 54%. The value of the Young's modulus determined previously by Boudou et al. for PAH/PGA multilayers in the wet state was (118 ± 34) kPa.[19] To our knowledge, the dry state stiffness of PAH/PGA films was not published before.

Figure 5 and Table 2 summarize the results obtained from wrinkling metrology method and the colloidal probe atomic force microscopy technique and from FTIR − ATR experiments. By increasing x, $(PAH/PGA_x\text{-}PSS_{1-x})_n$ films become softer with an elastic modulus 2 orders of magnitude smaller for $x \geq 0.75$ compared to $x \leq 0.5$. Thus, the elastic properties of $(PAH/PGA_x\text{-}PSS_{1-x})_n$ multilayer films can be tailored over a wide range only by changing the monomer molar fraction of PGA in the polyanion solution from 0.5 to 0.75 (Figure 5).

Figure 6 and Table 2 show the dependence of Young's modulus of the blended PAH/PGA−PSS film as a function of the monomer molar fraction of PGA in the film, fitted by a linear function for $0.1 < x < 1$. In the region where the PGA fraction in the film is lower or equal to 0.5, the E-modulus remains nearly constant and resides around 0.7 GPa (Figure 6). Despite the preferential incorporation of PGA over PSS in this region (Figure 2), the major fraction of polyanion present in the film is PSS leading to its significant contribution to the elastic properties of the film. When the molar fraction of PGA in the film increases from 0.5 to 1, the elastic modulus of the film decreases linearly until a plateau at around 6×10^{-3} GPa from x = 0.8. Thus, the elastic properties of $(PAH/PGA_x\text{-}PSS_{1-x})_n$ multilayer films evolves linearly with the molar fraction of PGA in the film between 0.5 and 0.8. The small amount of water inside PSS/PAH films (25%)[64] could explain the high Young's Modulus of pure PSS/PAH film. In contrary, PGA/PAH films shows a high water content in the film, about 40% according to the refractive index of pure PGA/PAH film equal to 1.47. This high hydration of the

Table 3. Young Modulus of $(PAH/PGA_x\text{-}PSS_{1-x})_n$ Multilayer Films for $x = 0.71$ and 0.73 As Measured by Wrinkling Metrology and Colloidal Probe AFM

	Young's modulus ($\times$ 10^{-1} GPa)		
	$x = 0.71$	$x = 0.73$	RH (%)
WM	1.9 ± 0.7	1.4 ± 0.9	56
CP−AFM		2.2 ± 0.4	60
	5.1 ± 1.6	4.4 ± 1.4	50

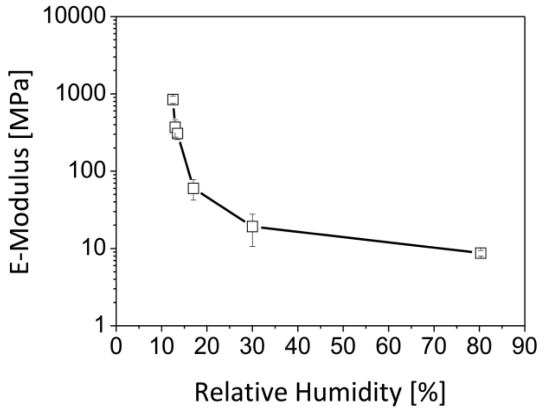

Figure 7. Evaluation of the elastic modulus E of the $(PAH/PGA_{0.88}\text{-}PSS_{0.12})_n$ multilayer films as a function of relative humidity as measured by CP−AFM in the humidity cell.

film could explain the lower Young modulus of pure PGA/PAH film compared to PSS/PAH. An increase in PGA in the blended film induces an increase of the film hydration and thus a decrease in Young's modulus of the film.

Overlap Regime: Comparison of AFM and Wrinkling Method Results. There is a regime in a range around $x = 0.7$ where both techniques can be applied to measure the elastic modulus. Therefore, we present a direct comparison of elastic constants in Table 3. These results demonstrate a good agreement between both methods. As expected, since AFM is on the limit of its applicability, errors of the AFM measurements are large. But the order of magnitude agrees with the wrinkling results, indicating that the results are method independent.

In order to determine how strong our system responds to the humidity changes, we performed experiments with the colloidal probe technique in a humidity cell under controlled humidity conditions. The measurements were performed on samples with $x = 0.88$.

Figure 7 shows that at higher humidities the elastic modulus increases slowly with decreasing humidity. The Young modulus changes from (8.7 ± 0.7) MPa to (19.2 ± 8.6) MPa when the RH decreases from 80 to 30%. Thus, the modulus value of (4.7 ± 1.6) MPa measured at 54% ambient humidity is in reasonable agreement with the modulus values obtained at controlled humidity (by comparing the modulus values between 80% and 30% RH), taking into consideration the uncertainties. At lower humidities, the modulus increases rapidly with the negligible changes in the humidity values. By reduction of the humidity from 17% to 13.5% to 12.5%, the modulus increases from (60.0 ± 17.8) MPa to (307.6 ± 51.2) MPa and to (843.7 ± 94.8) MPa.

The decrease of modulus with increasing humidity could be explained by the adsorption of water from vapor phase and corresponding swelling of a film. This happens due to the fact, that the PGA is very hydrophilic and can absorb much water from the vapor phase. In other words, the plastification effect takes place and water is a well-known plasticizer. Moreover, at different relative humidities the absorbed amount is different as was reported by Kuntz and Kauzmann.[65]

Similar swelling effects were reported before.[55,66−71] In most cases the reduced elastic modulus of LbL films in the swollen state was in the range 1−1000 MPa, and in dry state it is in the range 0.5−10 GPa.

Similar method was used to measure mechanical properties of LbL films in dry and swollen states by Lisunova et al.[72] For LbL film made of weak PE they found a 3−4-fold decrease of elastic modulus of a swollen state in comparison with dry state. In particular they got 700 ± 200 MPa for ambient air conditions and 0.2−4.3 MPa in liquid environment. This result is comparable to our system where swelling was done in water vapors and corresponding elastic modulus is in-between 10 and 1000 MPa.

SUMMARY AND CONCLUSIONS

In this study, we have investigated the mechanical properties of $(PAH/PGA_x\text{-}PSS_{1-x})_n$ multilayer films made from blended solutions of PGA and PSS. Using ATR-FTIR experiments, we first determined the relative composition in PGA and PSS inside the film as a function of x, the monomer molar fraction of PGA in the polyanion solution. We showed that with increasing the PGA molar fraction in the mixed PGA/PSS solution, the PGA molar fraction in the film increases almost linearly. To determine the elastic constants of $(PAH/PGA_x\text{-}PSS_{1-x})$, we used two different techniques: the wrinkling method and colloidal probe AFM. We found that with increasing the PGA molar fraction in the mixed solution, the blended film becomes softer and the elastic modulus becomes 2 orders of magnitude smaller for $x \geq 0.75$ compared to $x \leq 0.5$. This transition occurs at a mixing ratio of around $x = 0.7$. The elastic properties of $(PAH/PGA_x\text{-}PSS_{1-x})_n$ multilayer films can be tailored over a wide range from 0.7 GPa to 6 MPa only by changing monomer molar fraction of PGA in solution from 0.5 to 0.75. We also showed that for a given x the Young's modulus of the blended film strongly depends on the humidity changes as demonstrated by means of the colloidal probe AFM in a humidity cell under controlled humidity conditions. For $(PAH/PGA_{0.88}\text{-}PSS_{0.12})$ film, Young's modulus increases from hundreds of MPa at 12.5% RH to a few MPa at the 80% RH.

AUTHOR INFORMATION

Corresponding Author

*E-mail: (F.B.) fouzia.boulmedais@ics-cnrs.unistra.fr; (A.F.) Andreas.Fery@uni-bayreuth.de.

ACKNOWLEDGMENT

The research was financially supported by COST D 43. We thank Sina Rösler for the helpful assistance in carrying out of some experimental work and for the useful ideas. The authors are also thankful to Daria Andreeva (University of Bayreuth) for fruitful discussions. Eric Gonthier (Institut Charles Sadron, Strasbourg) is acknowledged for technical assistance with the FTIR measurements.

REFERENCES

(1) Decher, G.; Hong, J. D.; Schmitt, J. *Thin Solid Films* **1992**, *210* (1−2), 831–835.
(2) Jaber, J. A.; Schlenoff, J. B. *Curr. Opin. Colloid Interface Sci.* **2006**, *11* (6), 324–329.
(3) Mamedov, A. A.; Kotov, N. A. *Langmuir* **2000**, *16* (13), 5530–5533.
(4) Farhat, T. R.; Schlenoff, J. B. *Electrochem. Solid State Lett.* **2002**, *5* (4), B13–B15.
(5) Andreeva, D. V.; Fix, D.; Möhwald, H.; Shchukin, D. G. *Adv. Mater.* **2008**, *20* (14), 2789–2794.
(6) Jiang, C. Y.; Markutsya, S.; Tsukruk, V. V. *Adv. Mater.* **2004**, *16* (2), 157–161.
(7) Mallwitz, F.; Laschewsky, A. *Adv. Mater.* **2005**, *17* (10), 1296–1299.
(8) Lavalle, P.; Boulmedais, F.; Ball, V.; Mutterer, J.; Schaaf, P.; Voegel, J. C. *J. Membr. Sci.* **2005**, *253* (1−2), 49–56.
(9) Nolte, M.; Fery, A. *IEE Proc.-Nanobiotechnol.* **2006**, *153* (4), 112–120.
(10) Ott, P.; Trenkenschuh, K.; Gensel, J.; Fery, A.; Laschewsky, A. *Langmuir* **2010**, *26* (23), 18182–18188.
(11) Nolte, M.; Donch, I.; Fery, A. *ChemPhysChem* **2006**, *7* (9), 1985–1989.
(12) Sukhorukov, G.; Fery, A.; Möhwald, H. *Prog. Polym. Sci.* **2005**, *30* (8−9), 885–897.
(13) Johnston, A. P. R.; Cortez, C.; Angelatos, A. S.; Caruso, F. *Curr. Opin. Colloid Interface Sci.* **2006**, *11* (4), 203–209.
(14) Shiratori, S. S.; Rubner, M. F. *Macromolecules* **2000**, *33* (11), 4213–4219.
(15) Burke, S. E.; Barrett, C. J. *Biomacromolecules* **2003**, *4* (6), 1773–1783.
(16) Ladam, G.; Schaad, P.; Voegel, J. C.; Schaaf, P.; Decher, G.; Cuisinier, F. *Langmuir* **2000**, *16* (3), 1249–1255.
(17) Sui, Z. J.; Salloum, D.; Schlenoff, J. B. *Langmuir* **2003**, *19* (6), 2491–2495.
(18) Richert, L.; Boulmedais, F.; Lavalle, P.; Mutterer, J.; Ferreux, E.; Decher, G.; Schaaf, P.; Voegel, J. C.; Picart, C. *Biomacromolecules* **2004**, *5* (2), 284–294.
(19) Boudou, T.; Crouzier, T.; Auzely-Velty, R.; Glinel, K.; Picart, C. *Langmuir* **2009**, *25* (24), 13809–13819.
(20) Senger, B.; Francius, G.; Hemmerle, J.; Ball, V.; Lavalle, P.; Picart, C.; Voegel, J. C.; Schaaf, P. *J. Phys. Chem. C* **2007**, *111* (23), 8299–8306.
(21) Ott, P.; Gensel, J.; Roesler, S.; Trenkenschuh, K.; Andreeva, D.; Laschewsky, A.; Fery, A. *Chem. Mater.* **2010**, *22* (11), 3323–3331.
(22) Steitz, R.; Jaeger, W.; von Klitzing, R. *Langmuir* **2001**, *17* (15), 4471–4474.
(23) Qu, D.; Pedersen, J. S.; Garnier, S.; Laschewsky, A.; Möhwald, H.; von Klitzing, R. *Macromolecules* **2006**, *39* (21), 7364–7371.
(24) Nolte, A. J.; Cohen, R. E.; Rubner, M. F. *Macromolecules* **2006**, *39* (14), 4841–4847.
(25) Hübsch, E.; Ball, V.; Senger, B.; Decher, G.; Voegel, J. C.; Schaaf, P. *Langmuir* **2004**, *20* (5), 1980–1985.
(26) Debreczeny, M.; Ball, V.; Boulmedais, F.; Szalontai, B.; Voegel, J. C.; Schaaf, P. *J. Phys. Chem. B* **2003**, *107* (46), 12734–12739.
(27) Cho, J. H.; Quinn, J. F.; Caruso, F. *J. Am. Chem. Soc.* **2004**, *126* (8), 2270–2271.
(28) Quinn, J. F.; Yeo, J. C. C.; Caruso, F. *Macromolecules* **2004**, *37* (17), 6537–6543.
(29) Sun, J.; Wang, L. Y.; Gao, J.; Wang, Z. Q. *J. Colloid Interface Sci.* **2005**, *287* (1), 207–212.
(30) Francius, G.; Hemmerle, J.; Voegel, J. C.; Schaaf, P.; Senger, B.; Ball, V. *Langmuir* **2007**, *23* (5), 2602–2607.
(31) Quinn, A.; Tjipto, E.; Yu, A. M.; Gengenbach, T. R.; Caruso, F. *Langmuir* **2007**, *23* (9), 4944–4949.
(32) Li, Q.; Quinn, J. F.; Caruso, F. *Adv. Mater.* **2005**, *17* (17), 2058–2062.
(33) Benkirane-Jessel, N.; Lavalle, P.; Hübsch, E.; Holl, V.; Senger, B.; Haikel, Y.; Voegel, J. C.; Ogier, J.; Schaaf, P. *Adv. Funct. Mater.* **2005**, *15* (4), 648–654.
(34) Dubreuil, F.; Elsner, N.; Fery, A. *Eur. Phys. J. E* **2003**, *12* (2), 215–221.
(35) Gao, C.; Donath, E.; Moya, S.; Dudnik, V.; Möhwald, H. *Eur. Phys. J. E* **2001**, *5* (1), 21–27.
(36) Ballt, V.; Bernsmann, F.; Betscha, C.; Maechling, C.; Kauffmann, S.; Sengert, B.; Voegel, J. C.; Schaaf, P.; Benkirane-Jesselt, N. *Langmuir* **2009**, *25* (6), 3593–3600.
(37) Nolte, M.; Schoeler, B.; Peyratout, C. S.; Kurth, D. G.; Fery, A. *Adv. Mater.* **2005**, *17* (13), 1665–1669.
(38) Schlenoff, J. B.; Dubas, S. T.; Farhat, T. *Langmuir* **2000**, *16* (26), 9968–9969.
(39) Izquierdo, A.; Ono, S. S.; Voegel, J. C.; Schaaf, P.; Decher, G. *Langmuir* **2005**, *21* (16), 7558–7567.
(40) Born, M.; Wolf, E., *Principles of Optics*, 5th ed.; Pergamon: New York, 1975.
(41) Nolte, A. J.; Rubner, M. F.; Cohen, R. E. *Macromolecules* **2005**, *38* (13), 5367–5370.
(42) Butt, H. J. *Biophys. J.* **1991**, *60* (4), 777–785.
(43) Ducker, W. A.; Senden, T. J.; Pashley, R. M. *Nature* **1991**, *353* (6341), 239–241.
(44) Hutter, J. L.; Bechhoefer, J. *Rev. Sci. Instrum.* **1993**, *64* (7), 1868–1873.
(45) Greenspan, L. *J. Res. Natl. Bur. Stand. A: Phys. Chem.* **1976**, *81A* (1), 89–96.
(46) Young, J. F. *J. Appl. Chem. USSR* **1967**, *17* (9), 241.
(47) Lenormant, H.; Baudras, A.; Blout, E. R. *J. Am. Chem. Soc.* **1958**, *80* (23), 6192–6195.
(48) Koenig, J. L.; Frushour, B. *Biopolymers* **1972**, *11* (9), 1871.
(49) Jackson, M.; Haris, P. I.; Chapman, D. *J. Mol. Struct.* **1989**, *214*, 329–355.
(50) Yang, J. C.; Jablonsky, M. J.; Mays, J. W. *Polymer* **2002**, *43* (19), 5125–5132.
(51) Zundel, G., *Hydration and Intermolecular Interaction*. Academic Press: New York, 1969.
(52) Orler, E. B.; Yontz, D. J.; Moore, R. B. *Macromolecules* **1993**, *26* (19), 5157–5160.
(53) Stafford, C. M.; Harrison, C.; Beers, K. L.; Karim, A.; Amis, E. J.; Vanlandingham, M. R.; Kim, H. C.; Volksen, W.; Miller, R. D.; Simonyi, E. E. *Nat. Mater.* **2004**, *3* (8), 545–550.
(54) Aamer, K. A.; Stafford, C. M.; Richter, L. J.; Kohn, J.; Becker, M. L. *Macromolecules* **2009**, *42* (4), 1212–1218.
(55) Jiang, C. Y.; Wang, X. Y.; Gunawidjaja, R.; Lin, Y. H.; Gupta, M. K.; Kaplan, D. L.; Naik, R. R.; Tsukruk, V. V. *Adv. Funct. Mater.* **2007**, *17* (13), 2229–2237.
(56) Hendricks, T. R.; Lee, I. *Nano Lett.* **2007**, *7* (2), 372–379.
(57) Senger, B.; Francius, G.; Hemmerle, J.; Ohayon, J.; Schaaf, P.; Voegel, J. C.; Picart, C. *Microsc. Res. Tech.* **2006**, *69* (2), 84–92.
(58) Radmacher, M.; Domke, J. *Langmuir* **1998**, *14* (12), 3320–3325.
(59) Van Landingham, M. R. *Microsc. Today* **1997**, *97*, 12.
(60) Hertz, H. J. *J. Reine Angew. Math.* **1881**, *92*, 156–171.
(61) Lin, D. C.; Horkay, F. *Soft Matter* **2008**, *4* (4), 669–682.
(62) Schoeler, B.; Delorme, N.; Doench, I.; Sukhorukov, G. B.; Fery, A.; Glinel, K. *Biomacromolecules* **2006**, *7* (6), 2065–2071.
(63) Uricanu, V. I.; Duits, M. H. G.; Mellema, J. *Langmuir* **2004**, *20* (12), 5079–5090.
(64) Boulmedais, F.; Ball, V.; Schwinte, P.; Frisch, B.; Schaaf, P.; Voegel, J. C. *Langmuir* **2003**, *19* (2), 440–445.
(65) Kuntz, I. D.; Kauzmann, W. *Adv. Protein Chem.* **1974**, *28*, 239–345.
(66) Gunawidjaja, R.; Jiang, C. Y.; Peleshanko, S.; Ornatska, M.; Singamaneni, S.; Tsukruk, V. V. *Adv. Funct. Mater.* **2006**, *16* (15), 2024–2034.
(67) Elsner, N.; Kozlovskaya, V.; Sukhishvili, S. A.; Fery, A. *Soft Matter* **2006**, *2* (11), 966–972.
(68) Lavalle, P.; Voegel, J. C.; Vautier, D.; Senger, B.; Schaaf, P.; Ball, V. *Adv. Mater.* **2011**, *23* (10), 1191–1221.
(69) Kotov, N. A.; Podsiadlo, P.; Arruda, E. M.; Kheng, E.; Waas, A. M.; Lee, J.; Critchley, K.; Qin, M.; Chuang, E.; Kaushik, A. K.; Kim, H. S.; Qi, Y.; Noh, S. T. *ACS Nano* **2009**, *3* (6), 1564–1572.

(70) Bartkowiak, A.; Hunkeler, D. *Chem. Mater.* **1999**, *11* (9), 2486–2492.
(71) Kharlampieva, E.; Kozlovskaya, V.; Gunawidjaja, R.; Shevchenko, V. V.; Vaia, R.; Naik, R. R.; Kaplan, D. L.; Tsukruk, V. V. *Adv. Funct. Mater.* **2010**, *20* (5), 840–846.
(72) Tsukruk, V. V.; Lisunova, M. O.; Drachuk, I.; Shchepelina, O. A.; Anderson, K. D. *Langmuir* **2011**, *27* (17), 11157–11165.